Journal of Zhejiang University-SCIENCE A (Applied Physics & Engineering)
ISSN 1673-565X (Print); ISSN 1862-1775 (Online)
www.jzus.zju.edu.cn; www.springerlink.com
E-mail: jzus@zju.edu.cn

# Role of the pore-size distribution function on water flow in unsaturated soil*

Qian ZHAI[1,2], Harianto RAHARDJO[†‡2], Alfrendo SATYANAGA[2], PRIONO[2], Guo-liang DAI[1]

[1]*The State Key Laboratory for Reinforcement Concrete and Prestress Reinforcement Concrete Structures of the Ministry of Education, Southeast University, Nanjing 210096, China*

[2]*School of Civil and Environmental Engineering, Nanyang Technological University, Singapore 639798, Singapore*

[†]E-mail: chrahardjo@ntu.edu.sg

Received June 3, 2018; Revision accepted Oct. 11, 2018; Crosschecked Nov. 27, 2018

**Abstract:** The hydraulic properties of soil (i.e. soil-water characteristic curve (SWCC) and coefficient of permeability) govern the moisture flow in it. Previous research has indicated that the hydraulic properties of soil are dependent on its pore-size distribution. An improved capillary model is now proposed to explain the concept of the pore-size distribution in soil and its relationship to SWCC. A new model, the "valve model", is also proposed as the explanation for water flow in unsaturated soil. The pore-size distribution function is incorporated in the "valve model" and is used to calculate the relative coefficient of permeability for unsaturated soil. In this paper, the role of the pore-size distribution function in the estimation of SWCC and the permeability function are explained. Equations are proposed for estimating the pore-size distribution function from the experimental data of relative coefficient of permeability. The results from the proposed equations agree with the experimental data from laboratory measurement and published data.

**Key words:** Soil-water characteristic curve (SWCC); Hydraulic properties; Permeability function; Valve model; Pore-size distribution function

https://doi.org/10.1631/jzus.A1800347 **CLC number:** TU42; P66; P67

## 1 Introduction

The flow of fluids through soils is of great significance in the fields of geotechnical engineering, oil technology, and agriculture, etc. The hydraulic properties of unsaturated soil (including the soil-water characteristic curve (SWCC) and the permeability function) are governing factors that control moisture flow in it. Determination of the hydraulic properties of soil, including direct method such as laboratory or field measurement and indirect method such as estimation from the index properties of soil, is important in assessing the amount of seepage through underground soil.

Multi-fluid flow processes in soil are governed by geometrical pore-space characteristics (Tuli et al., 2005). Therefore, pore-size distribution in soil plays an important role in water movements in soil such as water drainage from (or storage in) the soil (to be represented as a soil-water characteristic curve) and water flow through the soil layer (to be represented as a permeability function). Vogel (1997) and Wildenschild et al. (2005) showed that the lack of knowledge concerning the control of water flow by pore geometry and of transport in soil had led to an incidental microscopic study of water flow and transport properties and shown them to be a function

‡ Corresponding author

* Project supported by the National Natural Science Foundation of China (No. 51878160), the National Key Research and Development Program of China (No. 2017YFC00703408), and the Fundamental Research Funds for the Central Universities (No. 2242018K41046), China

ORCID: Qian ZHAI, https://orcid.org/0000-0003-4619-2821

of geometrical pore-space properties. In this paper, microscopic studies on the pores inside the soil were carried out so as to understand the principle of water flow in unsaturated soil.

The object of this paper is to explain the role of the pore-size distribution function on the results of SWCC and permeability function. It is found that the pore-size distribution function acts as a bridge to convert SWCC into a permeability function, and vice versa. A mathematical equation is also proposed to estimate the pore-size distribution function from the experimental permeability data.

## 2 Literature review

The SWCC or soil water retention curve defines the relationship between water content (can be expressed in the forms of gravimetric water content, volumetric water content, or degree of saturation) in the soil and the soil suction. SWCC is an effective interpretive model that uses the elementary capillary model to provide an understanding of the distribution of water in the voids (Fredlund and Rahardjo, 1993; Fredlund et al., 2012). In addition, Childs and Collis-George (1950), Zhai and Rahardjo (2015), and Zhai et al. (2018a) recommended that SWCC should be considered as analogous to the pore-size distribution function. Therefore, SWCC can provide information on pore-size distribution in soil (i.e. the pore-size distribution function).

SWCC is expressed using a continuous mathematical equation which is commonly referred to as the SWCC best-fit equation. Various forms of SWCC best-fit equations have been proposed (Gardner, 1958; Brooks and Corey, 1964; van Genuchten, 1980; Fredlund and Xing, 1994; Kosugi, 1994; Pedroso et al., 2009). Fredlund and Xing (1994) adopted the concept of pore-size distribution and proposed a best-fit equation by integration of the pore-size distribution function. Leong and Rahardjo (1997) and Zapata (1999) concluded that Fredlund and Xing (1994)'s equation performed best in best fitting the SWCC data for a wide range of soil over the entire range of matric suction. In addition, Zapata (1999) also suggested that van Genuchten (1980)'s model could perform well for best fitting fine-grained soils. Therefore, both van Genuchten (1980)'s model and Fredlund and Xing (1994)'s equation are selected here to describe the pore-size distribution in soil. Expressing SWCC equations in the form of degree of saturation, both Fredlund and Xing (1994)'s equation and van Genuchten (1980)' model can be expressed in the form of degree of saturation, respectively, as follows:

$$\begin{aligned} S &= C(\psi)\frac{1}{\left\{\ln\left[\mathrm{e}+(\psi/a_{\mathrm{f}})^{n_{\mathrm{f}}}\right]\right\}^{m_{\mathrm{f}}}} \\ &= \left(1-\frac{\ln(1+\psi/C_{\mathrm{r}})}{\ln(1+10^{6}/C_{\mathrm{r}})}\right)\frac{1}{\left\{\ln\left[\mathrm{e}+(\psi/a_{\mathrm{f}})^{n_{\mathrm{f}}}\right]\right\}^{m_{\mathrm{f}}}}, \end{aligned} \tag{1}$$

where $S$ is the degree of saturation, $C(\psi)$ is correction function, $\psi$ is the matric suction, $C_{\mathrm{r}}$ is the input value, a roughly estimation of the residual suction, and Fredlund and Xing (1994) and Zhai and Rahardjo (2012a, 2012b) recommended that $C_{\mathrm{r}}$=1500 kPa for most cases, e is Euler's number, and $a_{\mathrm{f}}$, $n_{\mathrm{f}}$, and $m_{\mathrm{f}}$ are fitting parameters.

$$\Theta = \frac{S-S_{\mathrm{r}}}{1-S_{\mathrm{r}}} = \left[\frac{1}{1+(a_{\mathrm{v}}h)^{b_{\mathrm{v}}}}\right]^{c_{\mathrm{v}}}, \tag{2}$$

where $\Theta$ is the normalized degree of saturation, and $S_{\mathrm{r}}$ is the residual saturation. Zhai et al. (2017b) recommended that $S_{\mathrm{r}}$ in van Genuchten (1980)'s model should be treated as a fitting parameter. $h$ is the pressure head, and $a_{\mathrm{v}}$, $b_{\mathrm{v}}$, and $c_{\mathrm{v}}$ are fitting parameters.

Lambe (1955) indicated that the permeability of soil was dependent on soil properties such as soil composition, degree of saturation, void ratio, pore fluid, and its structure (including grain size). Tuli and Hopmans (2004) found that both pore geometry (or pore size and shape) and size distribution (or space distribution) were the main factors determining the relationship between SWCC and permeability function (including hydraulic or air conductivity). Childs and Collis-George (1950) adopted the concept of the pore-size distribution function and derived an equation for estimating the coefficient of permeability of soil with respect to different degrees of saturation (or permeability function). Mualem (1976) assumed that the

simplified capillary tubesin Childs and Collis-George (1950)'s model have certain lengths and proposed a pore tortuosity-connectivity parameter to improve Childs and Collis-George (1950)'s method for the estimation of the permeability function. However, Mualem (1976) also indicated that there was no procedure available to determine this tortuosity-connectivity parameter and it could only be estimated empirically. On the other hand, Zhai et al. (2018a) recommended consider the changes in soil volume rather than using the empirical parameter (such as the tortuosity-connectivity parameter) to estimate the relative hydraulic conductivity. Therefore, the effect of tortuosity-connectivity on the permeability function is not considered in this study. Childs and Collis-George (1950)'s model has been improved and extended by Marshall (1958), Kunze et al. (1968), Fredlund et al. (1994), Zhai and Rahardjo (2015), Zhai et al. (2017a, 2017b), and Zhai et al. (2018b). Therefore, the relative coefficient of permeability (or permeability function) also contains information about the pore-size distribution in the soil. However, there is no valid method or equation that can be used to estimate the pore-size distribution function from the measured unsaturated permeability data. In this study, a mathematical equation is proposed to estimate the pore-size distribution function from the measurement data of permeability and the results from this equation agree with experimental data from SWCC measurement.

## 3 Theory

The limitations of the conventional capillary model are explained in this section. An improved capillary model for description of the pores in soil is introduced. The pore-size distribution function is incorporated in this improved capillary model. In addition, a new model, the "valve model", is proposed to explain water flow in unsaturated soil. With the new model, the relationship between the pore-size distribution function and the permeability function can be explained clearly.

### 3.1 Conventional capillary model

Millington and Quirk (1961) and Mualem (1976) presented that the conventional capillary model was based on the "bundle of cylindrical capillaries" (BCC). The BCC representation postulates that a portion of the interconnected cylindrical pores is completely liquid-filled at a given matric potential whereas larger pores are completely empty. The idealization of the soil pore space model for the ease of explaining some aspects of engineering behavior of unsaturated soil was later found, but this model introduced serious limitations in its general application to unsaturated soil mechanics (Fredlund and Rahardjo, 1993; Fredlund et al., 2012; Zhai et al., 2017c).

In general, the limitations of conventional capillary models can be summarized as follows:

1. There is only a single tube for a particular pore size, which cannot represent the pore-size density for different pore sizes.

2. The water height in the tube is based on the capillary height and the total water amount in all these tubes may not be consistent with the water amount in soil with changes in matric suction.

3. The water drainage through a tube is piston-like, either fully filled or fully empty, which cannot represent actual water movement in an irregular pore.

4. The tubes are not connected to each other. As a result, this model cannot be used to explain the water flow in unsaturated soil.

5. As the tubes are not connected to each other, no "ink-bottle" effect can be created and this makes the model incapable of explaining the wetting process in the soil.

### 3.2 Improved capillary model

To overcome the limitations of the conventional capillary model as explained in Section 3.1, a new capillary model is proposed. First, an irregular pore is simplified into a series of circular pores with different sizes as illustrated in Fig. 1. Second, on the cross-sectional area, there are numbers of circular pores with different radii, which are converted from different irregular pores (Fig. 2b). The number of circular pores with radius of $r$ is dependent on the pore-size density, $f(r)$, rather than on a single pore. In this case, the soil element illustrated in Fig. 2a can be simplified as Fig. 2b and a 3D perspective view of the simplified soil element is illustrated in Fig. 3.

In the simplified element, the length, the width, and the height of a soil element are set as 1. The porosity of soil can be defined by the total volume of these cylindrical tubes (or capillary tubes) $\sum V_{\text{tube}}$. As the width of soil element is defined as 1, the porosity of soil can also be defined as the area of circular pores on the cross-sectional area, $\sum A_{\text{pore}}$, as follows:

$$\sum A_{\text{pore}} = \sum_{i=1}^{N} n_i \pi r_i^2, \tag{3}$$

where $n_i$ is the total number of the pores with radius of $r_i$, $r_1$ is the maximum radius of a pore, $r_N$ is the minimum radius of a pore, and $N$ is the total number of the groups of pores.

The pore-size distribution function defines the ratio of the volume of pores with certain radius of $r_i$ to the total volume of pores, and that ratio is commonly defined as the pore-size density $f(r_i)$. Therefore, the pore-size density of pores with radius of $r_i$, $f(r_i)$, can be calculated as follows:

$$f(r_i) = \frac{n_i \pi r_i^2}{\sum_{i=1}^{N} n_i \pi r_i^2}. \tag{4}$$

This improved model can help to define the pore-size distribution function more clearly than the conventional capillary model. In addition, the volumes of pores in the element are consistent with the definition of porosity. As soil elements can be connected to each other, the cylindrical tubes can be assumed to be connected to each other. With random connectivity, the "ink-bottle" effect can be simulated. The detail of calculation of the "ink-bottle" effect can be found from Zhai et al. (2017c).

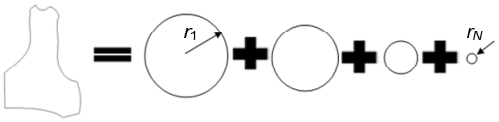


**Fig. 1 Simplification of an irregular pore into a series of circular pores**

### 3.3 Relationship between SWCC and the pore-size distribution function

If water fully fills the pores from $r_j$ to $r_N$, where $r_j$ is the maximum radius of a pore which is filled with water, then the degree of saturation in the soil can be calculated by

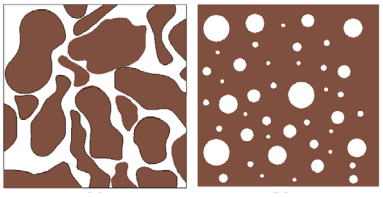


**Fig. 2 Simplification of pores in soil element**
(a) Irregular pores; (b) Simplified circular pores

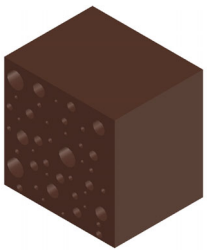

**Fig. 3 Illustration of capillary tubes in soil element**

$$S(\psi_j) = \frac{\sum_{i=j}^{N} n_i \pi r_i^2}{\sum_{i=1}^{N} n_i \pi r_i^2}. \tag{5}$$

It is observed that Eq. (5) can be obtained by the summation of Eq. (4) as follows:

$$S(\psi_j) = \sum_{i=j}^{N} f(r_i) = \frac{\sum_{i=j}^{N} n_i \pi r_i^2}{\sum_{i=1}^{N} n_i \pi r_i^2}. \tag{6}$$

Therefore, as illustrated in Eq. (6), SWCC expressed in the degree of saturation can be obtained from the integration of the pore-size distribution function. Eq. (6) gives the same conclusion from Fredlund and Xing (1994) namely that SWCC can be obtained by integrating the pore-size distribution function. Note that Eq. (6) was obtained based on the assumption that there is no soil volume change with changes in matric suction.

Therefore, the pore-size distribution function, $f(\psi)$, can be obtained by differentiation of the best fit equations (such as Eqs. (1) and (2)), which are expressed using the fitting parameters $a_{\text{f}}$, $n_{\text{f}}$, and $m_{\text{f}}$, or $a_{\text{v}}$, $b_{\text{v}}$, and $c_{\text{v}}$ as follows:

$$f(\psi)=\frac{\mathrm{d}S}{\mathrm{d}\lg(\psi)}$$
$$=\psi\ln(10)\left[\frac{m_{\mathrm{f}}n_{\mathrm{f}}\left(\psi/a_{\mathrm{f}}\right)^{n_{\mathrm{f}}-1}\left[1-\frac{\ln\left(1+\psi/C_{\mathrm{r}}\right)}{\ln\left(1+10^{6}/C_{\mathrm{r}}\right)}\right]}{a_{\mathrm{f}}\left[\mathrm{e}+\left(\psi/a_{\mathrm{f}}\right)^{n_{\mathrm{f}}}\right]\left\{\ln\left[\mathrm{e}+\left(\psi/a_{\mathrm{f}}\right)^{n_{\mathrm{f}}}\right]\right\}^{m_{\mathrm{f}}+1}}\right.$$
$$\left.+\frac{1}{\left[\ln\left(1+10^{6}/C_{\mathrm{r}}\right)\left(1+\psi/C_{\mathrm{r}}\right)\right]C_{\mathrm{r}}\left\{\ln\left[\mathrm{e}+\left(\psi/a_{\mathrm{f}}\right)^{n_{\mathrm{f}}}\right]\right\}^{m_{\mathrm{f}}}}\right], \tag{7}$$

$$f(h)=\frac{S-S_{\mathrm{r}}}{1-S_{\mathrm{r}}}$$
$$=(S_{\mathrm{r}}-1)h\ln(10)a_{\mathrm{v}}b_{\mathrm{v}}c_{\mathrm{v}}\left[\frac{1}{1+(a_{\mathrm{v}}h)^{b_{\mathrm{v}}}}\right]^{c_{\mathrm{v}}+1}(a_{\mathrm{v}}h)^{b_{\mathrm{v}}-1}. \tag{8}$$

### 3.4 Valve model for unsaturated permeability of soil

The water valve, as illustrated in Fig. 4a is commonly used in houses; it has the internal structural design illustrated in Fig. 4b. Its working mechanism is explained and illustrated in Fig. 5.

When the valve is fully opened, the cross-sectional area is completely open for water flow, as illustrated in Fig. 5a, the effective area that allows water to flow is $A_0$ and the water flow rate reaches its maximum value, $q_0$. When the valve is half opened, the effective cross-sectional area is reduced to $A_{\mathrm{i}}$ which results in a smaller flow rate, $q_{\mathrm{i}}$. When the valve is closed, the effective cross-sectional area becomes zero and the flow rate also reduces to zero. The flow rate $q_{\mathrm{i}}$ can be calculated from the ratio between $A_{\mathrm{i}}$ and $A_0$ as illustrated in Eq. (9). The reduction in the cross-sectional area can be calculated from the pore-size distribution function using the statistical method.

$$\frac{q_{\mathrm{i}}}{q_0}=\frac{A_{\mathrm{i}}}{A_0}. \tag{9}$$

The results of experimental work from Reinson et al. (2005) showed that water could flow only through the water phase and could not flow through the air phase. Assume two soil elements connect each other on section A-A, the water flow through the section is dependent on the moisture condition of the two pores as illustrated in Fig. 6. If both pores are wet (Fig. 6a), then water can flow across the section. On the other hand, if one pore is dry (Fig. 6b), then water is blocked by air and cannot flow across the section. The probability of the connection of two pores is dependent on the pore-size density of the pores.

In this case, if the effective area that allows water flow through the section can be calculated, then the relative coefficient of permeability can be calculated. By studying the effective area for each individual pore (from $r_m$ to $r_N$, where $r_m$ is the maximum radius of wet pore corresponding to matric suction of $\psi_m$), the total effective area on the cross-sectional area that allows water flow can be calculated as illustrated in Fig. 7, where $n$ is the porosity.

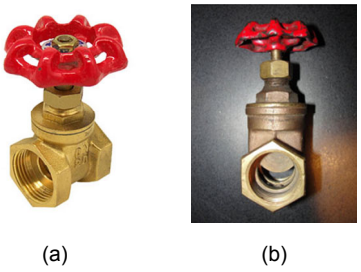


**Fig. 4 Illustration of water valve**
(a) Water valve; (b) Internal structure of water valve

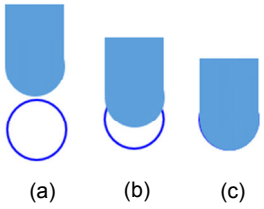


**Fig. 5 Illustration of working mechanism of a water valve**
(a) Valve is fully open; (b) Valve is half open; (c) Valve is fully closed

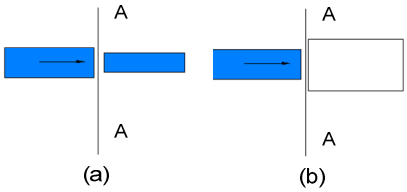


**Fig. 6 Illustration of water flow cross the section**
(a) Two pores are wet; (b) Big pore is dry

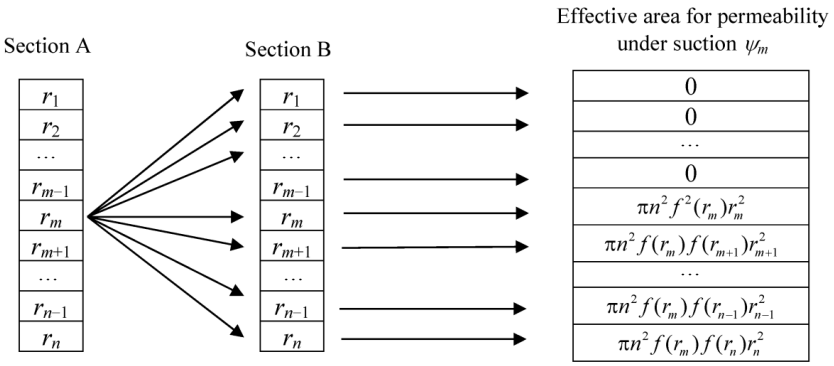


**Fig. 7 Illustration of effective area for each pore**

The summation of the effective areas under suction of $\psi_m$ can be divided by the total effective area under the fully saturated condition to determine the relative coefficient of permeability as shown in Eq. (10).

$$k_r=\left\{\left(S(\psi_m)-S(\psi_{m+1})\right)^2\psi_m^{-2}+\sum_{i=m+1}^{N}\left[\left(S(\psi_m)-S(\psi_i)\right)^2-\left(S(\psi_m)-S(\psi_{i-1})\right)^2\right]\psi_i^{-2}\right\}\Bigg/\left\{\sum_{i=1}^{N}\left[\left(1-S(\psi_i)\right)^2-\left(1-S(\psi_{i-1})\right)^2\right]\psi_i^{-2}\right\}, \tag{10}$$

where $k_r$ is the relative coefficient of permeability, and $S(\psi_m)$ is the degree of saturation corresponding to matric suction of $\psi_m$.

Substituting Fredlund and Xing (1994)'s equation into Eq. (10), the relative coefficient of permeability can be obtained using fitting parameters ($a_f$, $n_f$, and $m_f$) as shown in Eq. (11). In addition, if van Genuchten (1980)'s model is used as the SWCC best fit equation, the relative coefficient of permeability can be obtained using fitting parameters ($a_v$, $b_v$, and $c_v$) as shown in Eq. (13).

$$k_r=\frac{1}{A_{FX}}\left\{\left\{\frac{C(\psi_m)}{\left\{\ln\left[e+\left(\psi_m/a_f\right)^{n_f}\right]\right\}^{m_f}}-\frac{C(\psi_{m+1})}{\left\{\ln\left[e+\left(\psi_{m+1}/a_f\right)^{n_f}\right]\right\}^{m_f}}\right\}^2\frac{1}{\psi_m^2}+\sum_{j=m+1}^{N}\left\{\left\{\frac{C(\psi_m)}{\left\{\ln\left[e+\left(\psi_m/a_f\right)^{n_f}\right]\right\}^{m_f}}-\frac{C(\psi_j)}{\left\{\ln\left[e+\left(\psi_j/a_f\right)^{n_f}\right]\right\}^{m_f}}\right\}^2-\left\{\frac{C(\psi_m)}{\left\{\ln\left[e+\left(\psi_m/a_f\right)^{n_f}\right]\right\}^{m_f}}-\frac{C(\psi_{j-1})}{\left\{\ln\left[e+\left(\psi_{j-1}/a_f\right)^{n_f}\right]\right\}^{m_f}}\right\}^2\right\}\frac{1}{\psi_j^2}, \tag{11}$$

$$A_{FX}=\sum_{i=1}^{N}\left\{\left\{1-\frac{C(\psi_i)}{\left\{\ln\left[e+\left(\psi_i/a_f\right)^{n_f}\right]\right\}^{m_f}}\right\}^2-\left\{1-\frac{C(\psi_{i-1})}{\left\{\ln\left[e+\left(\psi_{i-1}/a_f\right)^{n_f}\right]\right\}^{m_f}}\right\}^2\right\}\frac{1}{\psi_i^2}, \tag{12}$$

where $A_{FX}$ is the effective area calculated using Fredlund and Xing (1994)'s equation when the soil is fully saturated.

$$k_r=\frac{1}{A_{VG}}\left\{\left\{\frac{1}{\left[1+(a_v\psi_m)^{b_v}\right]^{c_v}}-\frac{1}{\left[1+(a_v\psi_{m+1})^{b_v}\right]^{c_v}}\right\}^2\frac{1}{\psi_m^2}+\sum_{j=m+1}^{N}\left\{\left\{\frac{1}{\left[1+(a_v\psi_m)^{b_v}\right]^{c_v}}-\frac{1}{\left[1+(a_v\psi_j)^{b_v}\right]^{c_v}}\right\}^2\right.$$

$$-\left\{\frac{1}{\left[1+(a_{\mathrm{v}}\psi_m)^{b_{\mathrm{v}}}\right]^{c_{\mathrm{v}}}}-\frac{1}{\left[1+(a_{\mathrm{v}}\psi_{j-1})^{b_{\mathrm{v}}}\right]^{c_{\mathrm{v}}}}\right\}^2\left\{\frac{1}{\psi_j^2}\right\},\tag{13}$$

$$A_{\mathrm{VG}}=\sum_{i=1}^{N}\left\{\left\{1-\frac{1}{\left[1+(a_{\mathrm{v}}\psi_i)^{b_{\mathrm{v}}}\right]^{c_{\mathrm{v}}}}\right\}^2-\left\{1-\frac{1}{\left[1+(a_{\mathrm{v}}\psi_{i-1})^{b_{\mathrm{v}}}\right]^{c_{\mathrm{v}}}}\right\}^2\left\{\frac{1}{\psi_i^2}\right\},\right.\tag{14}$$

where $A_{\mathrm{VG}}$ is the effective area calculated using van Genuchten (1980)'s equation when the soil is fully saturated.

It is observed from Eqs. (1), (7), and (11) and Eqs. (2), (8), and (13) that SWCC, pore-size distribution function, $f(r)$, and relative coefficient of permeability, $k_{\mathrm{r}}$, can be expressed by the same set of fitting parameters (e.g. $a_{\mathrm{f}}$, $n_{\mathrm{f}}$, and $m_{\mathrm{f}}$ in Fredlund and Xing (1994)'s equation or $a_{\mathrm{v}}$, $b_{\mathrm{v}}$, and $c_{\mathrm{v}}$ in van Genuchten (1980)'s model). In this case, if any of these properties, SWCC, $f(r)$, or $k_{\mathrm{r}}$, is known, the other two properties can be calculated accordingly.

## 4 Experimental program for verification

Fredlund and Xing (1994) illustrated that SWCC and $f(r)$ can be calculated from each other. On the other hand, Zhai and Rahardjo (2015) and Zhai et al. (2017a, 2017b) demonstrated that $k_{\mathrm{r}}$ can be calculated from SWCC. However, it seems that there is no valid equation that can be used to estimate the pore-size distribution function from the measured permeability data. It is observed, however, that Eqs. (11) and (13) can be used to calculate SWCC from the experimental data of permeability. In order to verify the capability of Eqs. (11) and (13), one specimen of a compacted mixture of sand and kaolin K50S50 (50% sand with 50% kaolin) was prepared for both an unsaturated permeability test and SWCC measurement. The unsaturated permeability tests were carried out using an apparatus named unsaturated triaxial permeameter, which is modified from unsaturated triaxial equipment, as shown in Fig. 8. In this research, the modification followed the recommendations from Goh (2012), Goh et al. (2015), Priono (2016), and Rahimi and Rahardjo (2016).

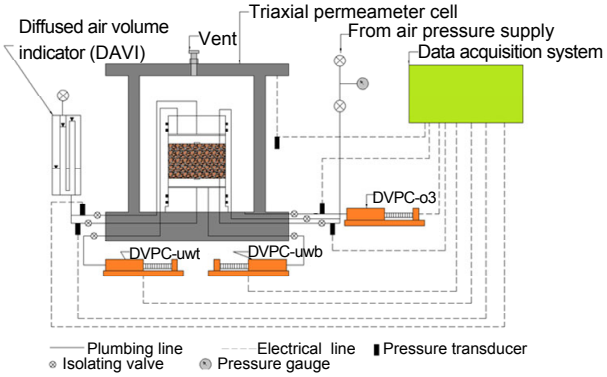


**Fig. 8 Schematic diagram of the unsaturated triaxial permeameter setup**

DVPC is the digital volume and pressure controller, uwt is the controlling top pore-water pressure, uwb denotes the controlling bottom pore-water pressure, and o3 denotes the controlling cell pressure

The unsaturated permeability measured was paused when a steady-state condition (or equilibrium condition) was achieved for a period of time. The equilibrium condition is usually determined from graphical observation. After the permeability test was completed at each suction stage, the equilibrium state was reached for the SWCC measurement. Following this procedure, the unsaturated permeability and SWCC could be measured simultaneously.

Index property tests were carried out on compacted specimens which were mixed by Ottawa sand (20–30 mesh) and L2-grade kaolin. Index properties of the soil samples used in this study are illustrated in Table 1.

**Table 1 Index properties of soils used in this study**

| Index property | Description |
|---|---|
| Dry density, $\rho_{\mathrm{d}}$ ($\times10^3$ kg/m$^3$) | 1.75 |
| Water content, $w$ (%) | 12.10 |
| Void ratio, $e$ | 0.48 |
| Liquid limit, LL (%) | 46.70 |
| Plastic limit, PL (%) | 27.40 |
| Plasticity index, PI (%) | 19.30 |
| Specific gravity, $G_{\mathrm{s}}$ | 2.59 |
| GSD–sand (%) | 50.00 |
| GSD–silt (%) | 37.50 |
| GSD–clay (%) | 12.50 |
| Unified soil classification system (USCS) | SM-ML |
| Saturated permeability, $k_{\mathrm{s}}$ (m/s) | $1.12\times10^{-8}$ |

Note: GSD represents the grain-size distribution data, and SM-ML represents the silty sand with low plasticity

In addition to the experimental measurements carried out in this study, another five sets of data including fine sand, volcanic sand, touchet silt loam, glass beads from Brooks and Corey (1964), and superstition sand from Richards (1952) were collected from different reports. As no index properties of these soils were reported in the literature, only the experimental data of the relative coefficient of permeability and SWCC for these soils are illustrated in Fig. 9.

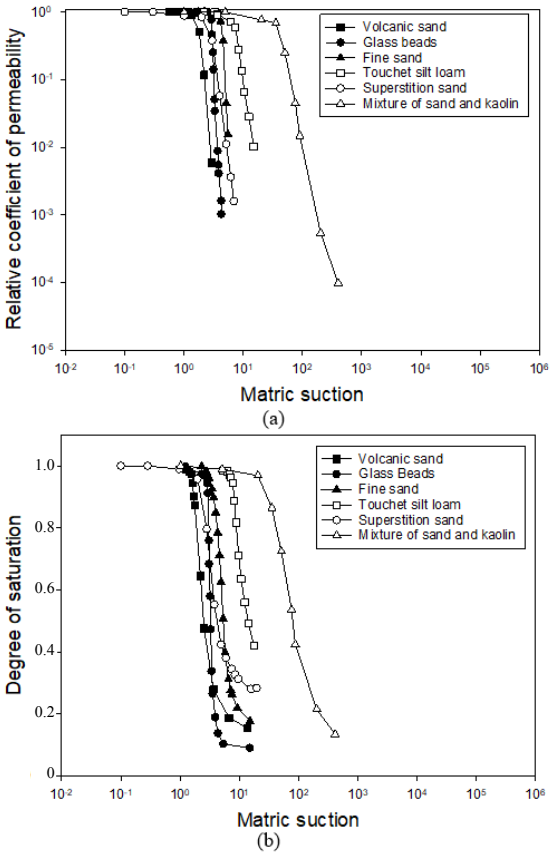


**Fig. 9 Experimental data of relative coefficient of permeability and SWCC of six types of soils permeameter setup: (a) measured relative coefficient of permeability; (b) measured SWCC**

Eqs. (11) and (13) were used to best fit the measured data of relative coefficients of permeability using curve fitting technique. After obtaining the fitting parameters in Fredlund and Xing (1994)'s equation (i.e., $a_f$, $n_f$, and $m_f$) and van Genuchten (1980)'s model ($a_v$, $b_v$, and $c_v$) from the regression procedure, these fitting parameters were then used to calculate SWCC. Consequently, the calculated SWCCs were compared with the measured SWCCs for these six types of soil.

## 5 Results and discussion

The fitting parameters such as $a_f$, $n_f$, and $m_f$ in Fredlund and Xing (1994)'s equation and $a_v$, $b_v$, and $c_v$ in van Genuchten (1980)'s model were obtained from the best fit procedure (by minimizing $\Sigma(\log(k_{ri})-\log(k'_{ri}))^2$, where $k_{ri}$ is the measured relative hydraulic conductivity and $k'_{ri}$ is the estimated relative hydraulic conductivity from Eq. (11) or Eq. (13)), which are as presented in Tables 2 and 3, respectively. The best fitting results for the relative hydraulic conductivity for these soils are illustrated in Fig. 10. Subsequently, the determined fitting parameters in Tables 2 and 3 were used to estimate the SWCC for these soils and the estimation results are illustrated in Fig. 11. The coefficients of goodness between the estimated results and the experimental results of SWCC for these soils are presented in Table 4.

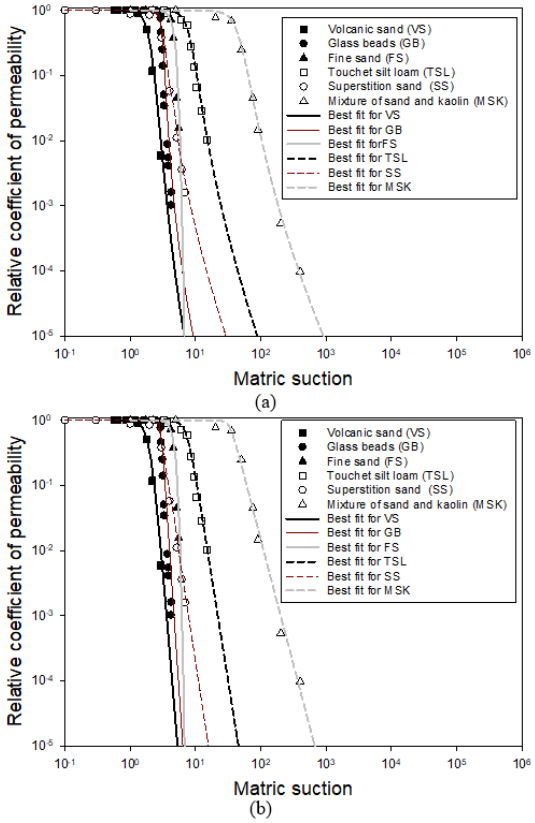


**Fig. 10 Best fitting results for these soils using Eq. (11) (a) and Eq. (13) (b)**

The results shown in Fig. 10 and Table 2 indicated that Eqs. (11) and (13) performed well (high values of $R^2$) as the best fit equations for the

**Table 2 Fitting parameters obtained by best fitting Eq. (11) on experimental data of relative coefficient of permeability**

| Soil | Fredlund and Xing (1994)'s equation | | | | |
|---|---|---|---|---|---|
| | $a_f$ (kPa) | $n_f$ | $m_f$ | $C_r$ (kPa) | $R^2$ |
| Volcanic sand | 2.10 | 6.34 | 2.02 | 1500 | 99.99% |
| Glass beads | 3.09 | 17.61 | 1.31 | 1500 | 97.73% |
| Fine sand | 6.27 | 8.57 | 12.99 | 1500 | 98.43% |
| Touchet silt loam | 7.76 | 6.38 | 0.76 | 1500 | 98.80% |
| Silty sand | 3.03 | 10.19 | 0.67 | 1500 | 99.78% |
| Mixture of sand and kaolin | 43.74 | 4.95 | 0.59 | 1500 | 99.77% |

**Table 3 Fitting parameters obtained by best fitting Eq. (13) on experimental data of relative coefficient of permeability**

| Soil | van Genuchten (1980)'s model | | | | |
|---|---|---|---|---|---|
| | $a_v$ (kPa$^{-1}$) | $b_v$ | $c_v$ | $\theta_r$ | $R^2$ |
| Volcanic sand | 0.487 | 6.76 | 0.740 | 0 | 99.99% |
| Glass beads | 0.342 | 31.93 | 0.200 | 0 | 97.06% |
| Fine sand | 0.157 | 8.61 | 5.490 | 0 | 98.42% |
| Touchet silt loam | 0.135 | 7.74 | 0.280 | 0 | 99.76% |
| Silty sand | 0.370 | 29.09 | 0.078 | 0 | 99.69% |
| Mixture of sand and kaolin | 0.030 | 11.31 | 0.081 | 0 | 99.22% |

$\theta_r$ is the residual volumetric water content

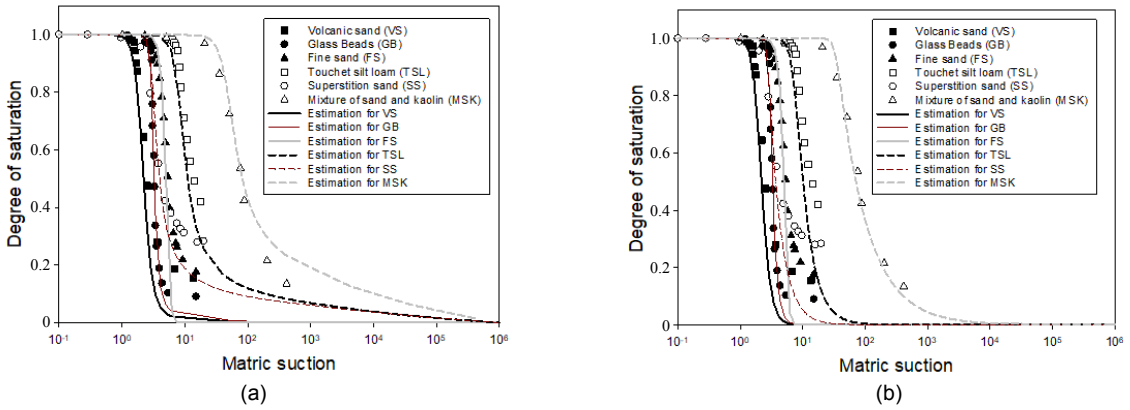


**Fig. 11 Estimation of SWCCs for the soils using fitting parameters $a_f$, $n_f$, and $m_f$ (a) and $a_v$, $b_v$, and $c_v$ (b)**

**Table 4 Coefficient of goodness, $R^2$, for the estimation of SWCC using Eqs. (11) and (13)**

| Soil | $R^2$ | |
|---|---|---|
| | Eq. (11) | Eq. (13) |
| Volcanic sand | 95.65% | 94.21% |
| Glass beads | 99.16% | 98.91% |
| Fine sand | 86.22% | 86.41% |
| Touchet silt loam | 95.22% | 87.97% |
| Silty sand | 95.70% | 83.71% |
| Mixture of sand and kaolin | 99.02% | 99.51% |

permeability function. The results illustrated in Fig. 11 and Table 3 indicated that the estimation results of SWCC from the measured data of relative coefficient of permeability also agreed with the measured data of SWCC.

## 6 Conclusions

The conventional capillary model was improved and a "valve model" was proposed to explain the water flow in unsaturated soil. The relationships between SWCC and pore-size distribution function, and between SWCC and permeability function could be well explained using the proposed models. It is observed that pore-size distribution function acts as a bridge to link SWCC and the permeability function. By best fitting the experimental data (including measured data in this study and published data collected from literature) with the proposed equations, the pore-size distribution function can be indirectly obtained from the measured permeability data.

Therefore, in the situation that only experimental data of relative coefficient of permeability are available, pore-size distribution function, $f(r)$, still can be indirectly obtained by using the equations proposed in this study.

## References


Brooks RH, Corey AT, 1964. Hydraulic Properties of Porous Media. Colorado State University, Fort Collins, CO, USA.

Childs EC, Collis-George N, 1950. The permeability of porous materials. *Proceedings of the Royal Society A*: *Mathematical*, *Physical and Engineering Sciences*, 201(1066): 392-405. https://doi.org/10.1098/rspa.1950.0068

Fredlund DG, Rahardjo H, 1993. Soil Mechanics for Unsaturated Soils. Wiley, New York, USA.

Fredlund DG, Xing AQ, 1994. Equations for the soil-water characteristic curve. *Canadian Geotechnical Journal*, 31(3):521-532. https://doi.org/10.1139/t94-061

Fredlund DG, Xing AQ, Huang SY, 1994. Predicting the permeability function for unsaturated soils using the soil-water characteristic curve. *Canadian Geotechnical Journal*, 31(4):533-546. https://doi.org/10.1139/t94-062

Fredlund DG, Rahardjo H, Fredlund MD, 2012. Unsaturated Soil Mechanics in Engineering Practice. Wiley, New York, USA.

Gardner WR, 1958. Mathematics of isothermal water conduction in unsaturated soils. Proceedings of the 37th Annual Meeting of the Highway Research Board.

Goh SG, 2012. Hysteresis Effects on Mechanical Behavior of Unsaturated Soil. PhD Thesis, Nanyang Technological University, Singapore.

Goh SG, Rahardjo H, Leong EC, 2015. Modification of triaxial apparatus for permeability measurement of unsaturated soils. *Soils and Foundations*, 55(1):63-73. https://doi.org/10.1016/j.sandf.2014.12.005

Kosugi K, 1994. Three-parameter lognormal distribution model for soil water retention. *Water Resources Research*, 30(4):891-901. https://doi.org/10.1029/93WR02931

Kunze RJ, Uehara G, Graham K, 1968. Factors important in the calculation of hydraulic conductivity. *Soil Science Society of America Journal*, 32(6):760-765. https://doi.org/10.2136/sssaj1968.03615995003200060020x

Lambe TW, 1955. The permeability of compacted fine-grained soils. Symposium on Permeability of Soils, ASTM.

Leong EC, Rahardjo H, 1997. Review of soil-water characteristic curve equations. *Journal of Geotechnical and Geoenvironmental Engineering*, 123(12):1106-1117. https://doi.org/10.1061/(asce)1090-0241(1997)123:12(1106)

Marshall TJ, 1958. A relation between permeability and size distribution of pores. *Journal of Soil Science*, 9(1):1-8. https://doi.org/10.1111/j.1365-2389.1958.tb01892.x

Millington RJ, Quirk JP, 1961. Permeability of porous media. *Nature*, 183(4658):387-388. https://doi.org/10.1038/183387a0

Mualem Y, 1976. A new model for predicting the hydraulic conductivity of unsaturated porous media. *Water Resources Research*, 12(3):513-522. https://doi.org/10.1029/WR012i003p00513

Pedroso DM, Sheng DC, Zhao JD, 2009. The concept of reference curves for constitutive modelling in soil mechanics. *Computers and Geotechnics*, 36(1-2):149-165. https://doi.org/10.1016/j.compgeo.2008.01.009

Priono, 2016. Anisotropy in Hydraulic Properties of Unsaturated Soils. PhD Thesis, Nanyang Technological University, Singapore.

Rahimi A, Rahardjo H, 2016. New approach to improve soil-water characteristic curve to reduce variation in estimation of unsaturated permeability function. *Canadian Geotechnical Journal*, 53(4):717-725. https://doi.org/10.1139/cgj-2015-0199

Reinson JR, Fredlund DG, Wilson GW, et al., 2005. Unsaturated flow in coarse porous media. *Canadian Geotechnical Journal*, 42(1):252-262. https://doi.org/10.1139/t04-070

Richards LA, 1952. Water conducting and retaining properties of soils in relation to irrigation. Proceedings of International Symposium on Desert Research, p.523-546.

Tuli A, Hopmans JW, 2004. Effect of degree of fluid saturation on transport coefficients in disturbed soils. *European Journal of Soil Science*, 55(1):147-164. https://doi.org/10.1046/j.1365-2389.2002.00493.x-i1

Tuli A, Hopmans JW, Rolston DE, et al., 2005. Comparison of air and water permeability between disturbed and undisturbed soils. *Soil Science Society of America Journal*, 69(5):1361-1371. https://doi.org/10.2136/sssaj2004.0332

van Genuchten MT, 1980. A closed-form equation for predicting the hydraulic conductivity of unsaturated soils. *Soil Science Society of America Journal*, 44(5):892-898. https://doi.org/10.2136/sssaj1980.03615995004400050002x

Vogel HJ, 1997. Morphological determination of pore connectivity as a function of pore size using serial sections. *European Journal of Soil Science*, 48(3):365-377. https://doi.org/10.1111/j.1365-2389.1997.tb00203.x

Wildenschild D, Hopmans JW, Rivers ML, et al., 2005. Quantitative analysis of flow processes in a sand using synchrotron-based X-ray microtomography. *Vadose Zone Journal*, 4(1):112-126. https://doi.org/10.2136/vzj2005.0112

Zapata CE, 1999. Uncertainty in Soil-water Characteristic Curve and Impacts on Unsaturated Shear Strength Predictions. PhD Thesis, Arizona State University, Tempe, USA.

Zhai Q, Rahardjo H, 2012a. Determination of soil–water characteristic curve variables. *Computers and Geotechnics*, 42:37-43. https://doi.org/10.1016/j.compgeo.2011.11.010

Zhai Q, Rahardjo H, 2012b. Reply to the discussion by Bellia et al. on "Determination of soil–water characteristic curve

variables". *Computers and Geotechnics*, 45:151-152. https://doi.org/10.1016/j.compgeo.2012.03.008

Zhai Q, Rahardjo H, 2015. Estimation of permeability function from the soil-water characteristic curve. *Engineering Geology*, 199:148-156. https://doi.org/10.1016/j.enggeo.2015.11.001

Zhai Q, Rahardjo H, Satyanaga A, et al., 2017a. Effect of bimodal soil-water characteristic curve on the estimation of permeability function. *Engineering Geology*, 230:142-151. https://doi.org/10.1016/j.enggeo.2017.09.025

Zhai Q, Rahardjo H, Satyanaga A, 2017b. Effects of residual suction and residual water content on the estimation of permeability function. *Geoderma*, 303:165-177. https://doi.org/10.1016/j.geoderma.2017.05.019

Zhai Q, Rahardjo H, Satyanaga A, 2017c. Uncertainty in the estimation of hysteresis of soil-water characteristic curve. *Environmental Geotechnics*, in press. https://doi.org/10.1680/jenge.17.00008

Zhai Q, Rahardjo H, Satyanaga A, 2018a. Estimation of the air permeability function from the soil-water characteristic curve. *Canadian Geotechnical Journal*, in press. https://doi.org/10.1139/cgj-2017-0579

Zhai Q, Rahardjo H, Satyanaga A, 2018b. A pore-size distribution function based method for estimation of hydraulic properties of sandy soils. *Engineering Geology*, 246:288-292. https://doi.org/10.1016/j.enggeo.2018.09.031

## 中文概要

**题　目：孔径分布函数对水分在非饱和土体中迁移的作用**

**目　的：**了解孔径分布函数对水分在非饱和土体中迁移的影响，并提出相关数学模型，量化非饱和土体在不同吸力作用下的渗透系数。

**创新点：**从孔径分布函数出发探讨土体的工程性质，以日常生活中所用的阀门模型解释非饱和土体在不同吸力作用下的渗透系数。提出采用非饱和土渗透系数的实验数据，间接估算土体的孔径分布函数。

**方　法：**从物理模型推导相关数学公式，并用实验结果对数学公式进行验证。

**结　论：**孔径分布函数主导非饱和土的渗透系数；孔径分布函数是连接土体两大水力特性（包括水土特征曲线和渗流方程）的桥梁。孔径分布函数对水分在土体中迁移的作用可以用日常生活中使用的阀门模型简单描述。基于阀门模型，土体的孔径分布函数也可以由土体的非饱和渗透系数的相关实验数据间接估算得到。

**关键词：**水土特征曲线；水力特性；孔径分布函数；渗透方程；阀门模型